Rapid effects of acute anoxia on spindle kinetochore interactions activate the mitotic spindle checkpoint

Rahul Pandey*, Sebastian Heeger‡ and Christian F. Lehner§,¶

Department of Genetics, BZMB, University of Bayreuth, 95440 Bayreuth, Germany

*Present address: Institute of Medical Biology, 61 Biopolis Drive, 138673, Singapore
‡Present address: Cancer Research UK, 44 Lincoln's Inn Fields, London, WC2A 3PX, UK
§Present address: University of Zurich, Institute of Zoology, Winterthurerstrasse 190, 8057 Zürich, Switzerland
¶Author for correspondence (e-mail: christian.lehner@zool.uzh.ch)

Accepted 20 June 2007
Journal of Cell Science 120, 2807-2818 Published by The Company of Biologists 2007
doi:10.1242/jcs.007690

Summary

The dramatic chromosome instability in certain tumors might reflect a synergy of spindle checkpoint defects with hypoxic conditions. In *Caenorhabditis elegans* and *Drosophila melanogaster*, spindle checkpoint activation has been implicated in the response to acute anoxia. The activation mechanism is unknown. Our analyses in *D. melanogaster* demonstrate that oxygen deprivation affects microtubule organization within minutes. The rapid effects of anoxia are identical in wild-type and spindle checkpoint-deficient *Mps1* mutant embryos. Therefore, the anoxia effects on the mitotic spindle are not a secondary consequence of spindle checkpoint activation. Some motor, centrosome and kinetochore proteins (dynein, Kin-8, Cnn, TACC, Cenp-C, Nuf2) are rapidly relocalized after oxygen deprivation. Kinetochores congress inefficiently into the metaphase plate and do not experience normal pulling forces. Spindle checkpoint proteins accumulate mainly within the spindle midzone and inhibit anaphase onset. In checkpoint-deficient embryos, mitosis is still completed after oxygen deprivation, although accompanied by massive chromosome missegregation. Inhibitors of oxidative phosphorylation mimic anoxia effects. We conclude that oxygen deprivation impairs the chromosome segregation machinery more rapidly than spindle checkpoint function. Although involving adenosine triphosphate (ATP)-consuming kinases, the spindle checkpoint can therefore be activated by spindle damage in response to acute anoxia and protect against aneuploidies.

Key words: Hypoxia, Spindle checkpoint, Mps1, BubR1, Bub3, Cenp-C, Nuf2

Introduction

Oxygen plays a decisive role in metabolism and is particularly important in metazoans for efficient adenosine triphosphate (ATP) production by oxidative phosphorylation. Diverse and highly adapted mechanisms have evolved to cope with oxygen limitation during development and adult life.

A well-known pathway triggered by acute and chronic hypoxia involves the activation of the HIF-1 transcription factor. This pathway has been shown to operate in a conserved manner in vertebrates and invertebrates such as *Caenorhabditis elegans* and *Drosophila melanogaster* (Gorr et al., 2006). In addition, experiments with these invertebrate model organisms have revealed the importance of alternative pathways, especially in anoxia when oxygen levels are even further decreased. Not only nematode (Padilla et al., 2002) and insect embryos (Foe and Alberts, 1985) but also some vertebrates (Padilla and Roth, 2001) tolerate extended periods of anoxia. In response to anoxia, they enter a state of suspended animation from which they can rapidly recover upon reoxygenation. HIF-1 is not required in *C. elegans* for survival of anoxia, whereas it is clearly crucial for survival of hypoxia (Jiang et al., 2001; Padilla et al., 2002). However, a screen for *C. elegans* genes required for survival of anoxia has led to the identification of *san-1*, which encodes a homolog of budding yeast Mad3 (Nystul et al., 2003). Mad3 is a component of the mitotic spindle checkpoint, a surveillance pathway known to monitor the bipolar integration of chromosomes into the mitotic spindle. Moreover, experiments in *D. melanogaster* demonstrated that Mps1, which also functions in the spindle checkpoint, is required for the mitotic arrest caused by severe hypoxia (Fischer et al., 2004).

The mitotic spindle checkpoint acts during mitosis and prevents progression into anaphase until all kinetochores are attached to the mitotic spindle and under physical tension (for a review, see Musacchio and Salmon, 2007). Several proteins are known to function in the spindle checkpoint. Apart from the components introduced above (Mad3, Mps1), additional proteins are involved (Mad1, Mad2, Bub3, Bub1, BubR1). Mps1, Bub1 and BubR1 are protein kinases. In metazoans, the kinesin Cenp-E and the Rod/Zw10/Zwilch (RZZ) complex, which recruits dynein-dynactin and Mad2 to the kinetochore, have also been implicated in the spindle checkpoint. The molecular interactions that lead to spindle checkpoint activation are not yet understood in detail. However, it is clear that spindle checkpoint activity prevents Fzy/Cdc20-APC/C ubiquitin ligase from marking securin and B-type cyclins for rapid proteasomal degradation. Securin inhibits separase, a protease that cleaves the Scc1 subunit of the cohesin complex. Therefore, as long as the spindle checkpoint remains active, sister chromatids are kept together by the cohesin linkage and anaphase cannot proceed. Moreover, high levels of B-type cyclin cdk activity maintain the mitotic state in the spindle checkpoint arrest.

The spindle checkpoint protects against aneuploidies. Spindle checkpoint dysfunction has been proposed to be involved in tumor formation, because excessive chromosome instability is a hallmark of a large fraction of solid human tumors. Evidence supporting this notion is increasing (Kops et al., 2005). Moreover, the spindle checkpoint might be of particular importance in tumor cells because their growth is known to be severely constrained by oxygen limitation (Hockel and Vaupel, 2001; Pouyssegur et al., 2006). As a result, areas with very low (down to zero) oxygen partial pressures exist in solid tumors, occurring either acutely or chronically (Hockel and Vaupel, 2001). Based on the initial analyses in *C. elegans* and *D. melanogaster*, it is readily conceivable that it is the combination of spindle checkpoint dysfunction and severe hypoxia that contributes to the remarkable chromosome instability typically observed in tumor cells. At least in the two model organisms, this combination clearly results in mitotic chromosome segregation defects (Fischer et al., 2004; Nystul et al., 2003). A more detailed analysis of the functional connections between anoxia and the spindle checkpoint should therefore be of interest.

The synchronous cell cycle progression of thousands of nuclei that occurs during the syncytial blastoderm stage of early *Drosophila* embryogenesis provides many advantages for experimental studies. Zalokar and Erk already observed that anoxia leads to a rapid and reversible developmental arrest during these stages in wild type (Zalokar and Erk, 1976). The studies of Foe and Alberts (Foe and Alberts, 1985) and DiGregorio et al. (DiGregorio et al., 2001) clearly revealed that anoxia triggers chromatin condensation in interphase nuclei and blocks further cell cycle progression within a few minutes. Embryos that have already entered mitosis at the time of anoxia induction become arrested either in metaphase or in late telophase. A metaphase arrest is observed when anoxia is induced before the metaphase to anaphase transition, and a late telophase arrest thereafter (DiGregorio et al., 2001; Douglas et al., 2005; Douglas et al., 2001; Foe and Alberts, 1985). These studies have also established that induction of a mitotic arrest by anoxia is not specific to the early syncytial stages but a general response throughout development. This anoxia response might be important in nature because *D. melanogaster* deposit their eggs into fermenting yeast on decaying fruit where hypoxia is likely to be a frequent physiological condition encountered during development.

In principle, it is conceivable that the early and rapid activation of the mitotic spindle checkpoint in response to anoxia involves an unknown dedicated pathway directly targeting one of the spindle checkpoint components. Such a pathway would appear especially beneficial if the error-free execution of post-metaphase processes were to be more sensitive to oxygen shortage than the initial mitotic processes. In this case, spindle assembly and chromosome attachment might still occur normally after oxygen deprivation, but progression into a more oxygen-dependent anaphase could then be inhibited by a dedicated anoxia-sensing spindle checkpoint activation pathway. Alternatively, the process of chromosome attachment to the mitotic spindle might be highly sensitive to oxygen deprivation. In this case, the spindle checkpoint would be activated by free kinetochores or reduced tension between sister kinetochores. Our analyses support this latter notion. We demonstrate that spindle and kinetochore function are indeed very rapidly affected by oxygen deprivation, not just in wild-type but also in checkpoint-deficient *Mps1* mutant embryos. Crucial components of centrosomes and spindles as well as kinetochore proteins including Cenp-C, which was thought to localize exclusively and constitutively to the centromere, are rapidly and dramatically redistributed in response to anoxia.

Results

Anoxia has rapid effects on mitotic spindles

Previous analyses have demonstrated that oxygen deprivation from the normal 21% to below 2% triggers a rapid cell cycle arrest in syncytial *Drosophila* embryos (DiGregorio et al., 2001; Douglas et al., 2005; Douglas et al., 2001; Foe and Alberts, 1985). In the following, we will use the term anoxia for these conditions even though our experimental procedures do not eliminate oxygen completely. We use this term to clearly distinguish our relatively severe conditions from milder hypoxia (3-5% O_2), which is sufficient for HIF-1 activation but does not trigger rapid cell cycle and developmental arrest during *Drosophila* development (Lavista-Llanos et al., 2002).

Mitotic spindles and congressed chromosomes have been shown to be present in arrested syncytial embryos when anoxia is induced after entry into mitosis but before the metaphase to anaphase transition (DiGregorio et al., 2001; Douglas et al., 2001; Fischer et al., 2004). However, a careful comparison revealed that the mitotic spindles in arrested anoxic embryos that were fixed after 20 minutes of incubation in degassed buffer were different from metaphase spindles in normoxic embryos (Fig. 1A). After anti-α-tubulin labeling, centrosome staining was either reduced or not apparent in anoxic embryos. Moreover, asters were greatly reduced or absent. In addition, spindles were narrow and contained few and only short microtubule fibers that did not extend far away from the metaphase plates. The extent of these spindle abnormalities was somewhat variable. In the majority of the anoxic embryos, abnormalities were at least as severe as in the example shown in Fig. 1A.

To analyze how fast spindle abnormalities develop in anoxia, we fixed embryos after a two- or five-minute incubation in degassed buffer. Spindles were observed to be affected after two minutes of anoxia (Fig. 1A). After five minutes, abnormalities were more severe but still minor than after 20 minutes of anoxia. Apart from a partial centrosome detachment and a reduction of astral and centrosome-proximal spindle fibers (Fig. 1A), centrosome separation appeared to be slightly increased in anoxia (Fig. 1B).

To study the effects of anoxia on spindle behavior, we also performed in vivo imaging with embryos expressing green fluorescent protein (GFP)-α-tubulin (Grieder et al., 2000). These embryos were made anoxic by applying a flow of nitrogen (Fig. 1C) or argon gas (data not shown). As previously described (DiGregorio et al., 2001; Douglas et al., 2001), we observed a rapid mitotic arrest after oxygen deprivation during early mitosis. We were unable to observe clear spindle abnormalities after two minutes, in contrast to our findings with fixed embryos. Moreover, even after prolongation of anoxia up to 20 minutes, we never observed the almost complete elimination of spindles that was frequently apparent after 20 minutes of incubation in degassed buffer followed by fixation and anti-α-tubulin labeling. However, after prolonged

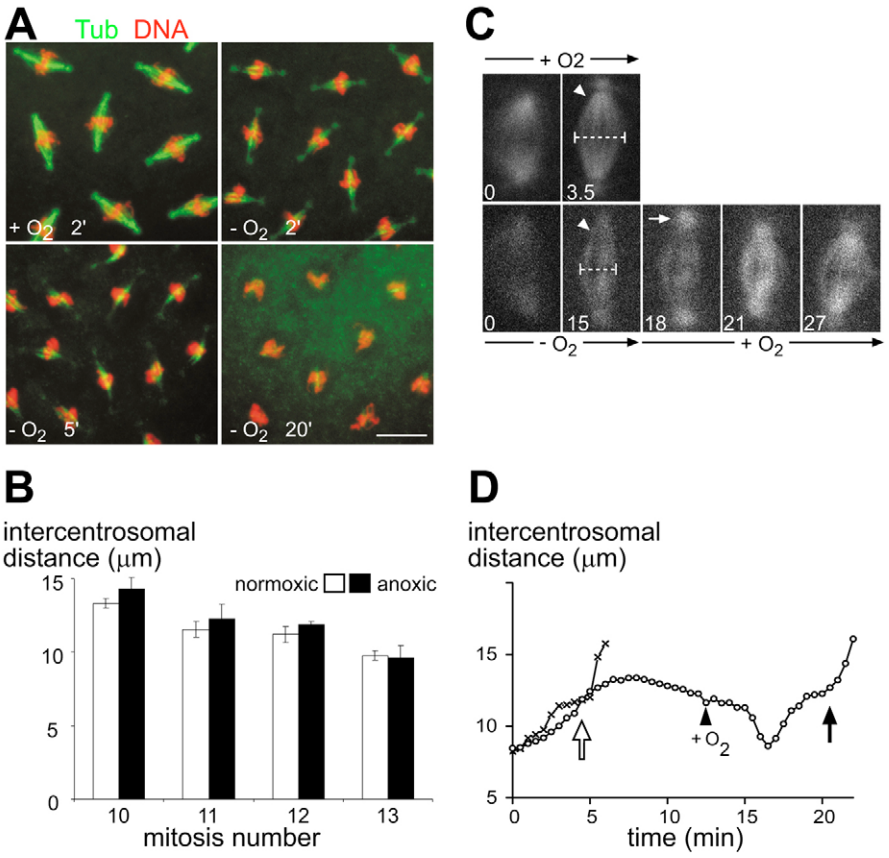

Fig. 1. Mitotic spindle organization in anoxia. (A) Early *Drosophila* embryos during the synchronous syncytial blastoderm cycles were incubated in either normoxic ($+O_2$) or anoxic ($-O_2$) buffer for 2, 5 or 20 minutes (2′, 5′, 20′) before fixation and labeling with anti-α-tubulin (Tub) and a DNA stain (DNA). Metaphase embryos reveal an increasing reduction of centrosome-proximal spindle fibers during anoxia. Bar, 10 μm. (B) The intercentrosomal distances in metaphase spindles (in μm on y-axis ± s.d.) after incubation (2 minutes) in either normoxic (white bars) or anoxic (black bars) buffer before fixation and immunolabeling (see A) was measured during mitosis 10, 11, 12 and 13. At least 25 different spindles from at least five different embryos were measured and averaged for each bar (*P* values obtained with *t*-test for mitoses 10, 11, 12 and 13 were 0.028, 0.2, 0.035 and 0.77). (C) Selected frames are shown after time-lapse in vivo imaging of embryos expressing α-tubulin-GFP. Time in minutes after prometaphase onset is indicated in the lower-left corners. In the presence of oxygen ($+O_2$, top row), the last metaphase frame is reached after 3.5 minutes, followed by anaphase (not shown). In the embryo made anoxic at the start of mitosis ($-O_2$, lower row), a metaphase arrest is maintained until after reoxygenation ($+O_2$, lower row). The last frame before reoxygenation at 15 minutes reveals the loss of centrosome-proximal spindle fibers (arrowheads) and a reduced spindle width (broken lines) in comparison with normoxic metaphase spindles. Reoxygenation is followed by a pronounced increase in centrosomal fibers (18 minutes, arrow) and spindle shortening (21 minutes) before an apparently normal metaphase spindle (27 minutes) precedes anaphase (not shown). (D) The intercentrosomal distance in mitotic spindles was determined after in vivo imaging of embryos expressing GFP-D-TACC starting in prophase. Anaphase onset in normoxic conditions (x-x) is indicated by the open arrow. During the metaphase arrest in anoxic conditions (o-o), the intercentrosomal distance extends slightly beyond normoxic metaphase values. Reoxygenation (indicated by arrowhead $+O_2$) is followed by a pronounced shortening and eventual anaphase onset (black arrow). The given distances at each time point are average values of five different spindles observed in representative embryos.

anoxia, the reduction of centrosome-proximal spindle fibers was also evident in the in vivo imaging experiments (Fig. 1C). A very similar spindle response to prolonged anoxia has also previously been observed using in vivo imaging of nonclaret disjunctional (Ncd)-GFP, a fluorescent spindle-associated *Drosophila* Kinesin-14 protein (Douglas et al., 2001; Sciambi et al., 2005). The apparent discrepancy between the extents of spindle abnormalities observed after our fixation and in vivo imaging experiments might be explained by the comparatively lower signal to noise ratio and lower spatial resolution of our in vivo imaging. Moreover, the methanol fixation applied in our experiments is known to disturb some aspects of the microtubule organization (Kellogg et al., 1988) and thus it might enhance the apparent defects.

In vivo imaging allowed an observation of spindle behavior during recovery from anoxia. Reoxygenation was followed by a prominent increase in the density of microtubules around centrosomes (Fig. 1C). Subsequently, the centrosomes were pulled towards the spindle, resulting in a distinct shortening of spindle length (Fig. 1C). Thereafter the spindle adopted an essentially normal metaphase appearance (Fig. 1C) followed rapidly by anaphase onset (not shown). In vivo imaging with embryos expressing the centrosomal protein GFP-D-TACC (Barros et al., 2005) confirmed the characteristic spindle shortening preceding anaphase during recovery from anoxia (Fig. 1D). Spindles shortened transiently to a length below that of normoxic metaphase spindles but comparable to prophase spindles. The defective poles of metaphase spindles in anoxic embryos therefore appear to be extensively rebuilt after reoxygenation.

The rapid spindle malfunction in response to oxygen deprivation is independent of the spindle checkpoint

To address whether the observed rapid effects of oxygen deprivation on the spindle might be cause or consequence of spindle checkpoint activation, we incubated checkpoint-deficient embryos lacking *Mps1* function (Fischer et al., 2004) for 5 minutes in degassed buffer followed by fixation and anti-α-tubulin labeling. Anoxic *Mps1* mutant embryos with metaphase plates (Fig. 2A, lower panel) were found to display the same abnormalities as observed with checkpoint-competent control embryos (Fig. 1A). Moreover, we emphasize that normoxic *Mps1* mutant embryos (Fig. 2A, upper panel) did not display the metaphase spindle abnormalities that are

characteristically observed in anoxic embryos. We conclude, therefore, that the rapid initial anoxia effects on spindle organization occur independent of *Mps1* function.

In vivo imaging of *Mps1* mutant embryos, in which completion of mitosis is not blocked by oxygen deprivation, allowed an analysis of the function of the mitotic apparatus in anoxia. To monitor chromosome congression and segregation, we used embryos expressing green fluorescent Cenp-A/Cid centromere protein and red fluorescent histone H2Av (Heeger et al., 2005). These experiments revealed that anoxia impaired chromosome congression during prometaphase. Congression proved to be slow and incomplete after oxygen deprivation, whereas it occurred far more effectively in normoxic *Mps1* mutants (Fig. 2B) (Fischer et al., 2004). Moreover, in anoxic *Mps1* mutant embryos, anaphase appeared to start with a delay but still before normal metaphase plates had formed (Fig. 2B). Anaphase was also significantly slower in anoxia. The leading centromeres moved towards the poles with an average speed of approximately 2.5 μm minute^{-1} in anoxic *Mps1* mutants compared with approximately 4 μm minute^{-1} in normoxic ones (in both cases s.d.=0.25 μm minute^{-1} and n=12 mitotic figures from a total of three different embryos). Consistent with the observed pronounced congression defects, lagging chromosomes were far more frequently observed during anaphase in anoxic compared with normoxic *Mps1* mutants (Fig. 2B) (Fischer et al., 2004). These observations suggest that spindle attachment of kinetochores is impaired by anoxia.

To analyze anoxia effects on spindle tension in *Mps1*$^{+}$ embryos, we compared the average separation of sister kinetochores in normoxic and anoxic metaphase plates after immunolabeling with antibodies against α-tubulin and Cenp-A/Cid (Fig. 2C). As previously established in cultured *Drosophila* cells and cellularized embryos (Heeger et al., 2005; Logarinho et al., 2004), chromosome biorientation in normoxic syncytial embryos was also found to be accompanied by an increase in the average separation of sister kinetochores, from 0.42 μm in prophase to 0.71 μm in metaphase (Fig. 2D). However, in anoxic metaphase plates, the average distance between sister kinetochores (0.63 μm) was slightly (12%) but significantly shorter than in the normoxic controls (Fig. 2D). Tension generated by the mitotic spindle or kinetochore attachment, therefore, appears to be reduced in anoxia. Apart from the reduced inter-sister kinetochore distances, the α-tubulin and Cenp-A/Cid double labeling also demonstrated that the anoxic spindles were largely composed of kinetochore microtubules that are known to be the most stable spindle fibers (McIntosh et al., 2002).

Effects of anoxia on centrosomal components and motor proteins

According to our microtubule analyses, the mitotic apparatus is rapidly affected by oxygen deprivation. Anoxia induction leads to a reduction of centrosome-proximal spindle fibers and centrosome detachment. Therefore, centrosomal components

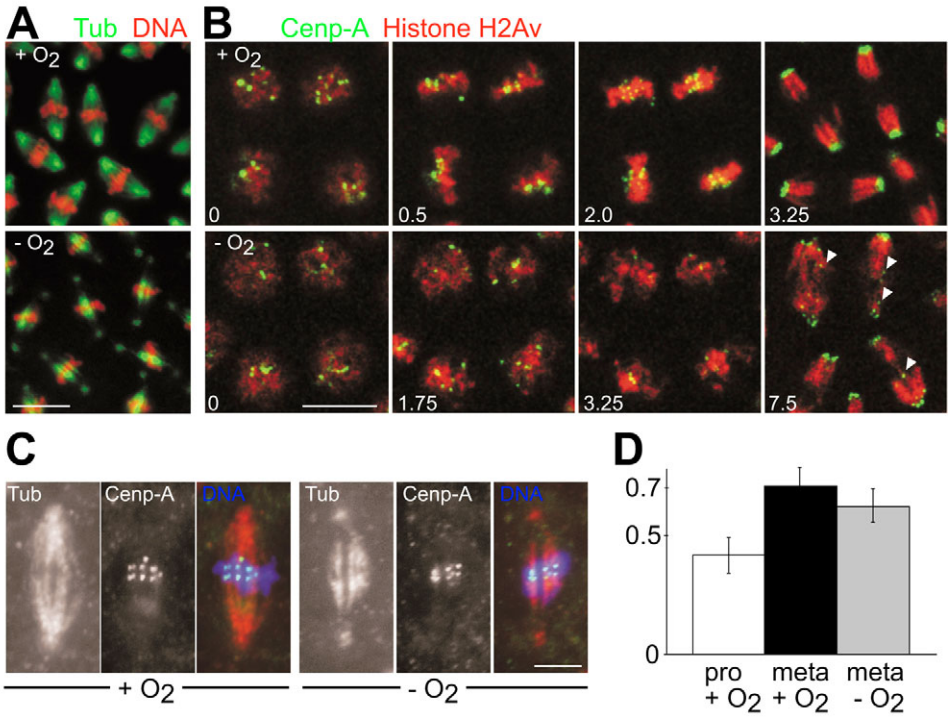

Fig. 2. Mitotic spindle function in anoxia. (A) Spindle checkpoint-deficient embryos lacking Mps1 protein kinase function were incubated during the synchronous syncytial blastoderm cycles in either normoxic (+O_2) or anoxic (–O_2) buffer for 5 minutes before fixation and labeling with anti-α-tubulin (Tub) and a DNA stain (DNA). The effects of anoxia on metaphase spindles do not depend on spindle checkpoint function (compare with Fig. 1A). Bar, 10 μm. (B) Progression through mitosis was analyzed by in vivo imaging of *Mps1* mutant embryos expressing a green fluorescent Cenp-A/Cid centromere protein (Cenp-A) and a red fluorescent histone H2A variant (Histone H2Av) in either normoxic (+O_2, top row) or anoxic (–O_2, bottom row) conditions. Time in minutes starting in early prometaphase is indicated in the lower-left corners of the selected frames. Chromosome congression in anoxia is slow and incomplete at the time of anaphase onset. Subsequent chromosome segregation is also slow. Some of the frequent lagging centromeres are indicated by arrowheads. Bar, 10 μm. (C,D) Spindle checkpoint-competent embryos were incubated during the synchronous syncytial blastoderm cycles in either normoxic (+O_2) or anoxic (–O_2) buffer for 5 minutes before fixation and labeling with antibodies against α-tubulin (Tub), Cenp-A (Cenp-A) and a DNA stain (DNA). The relative resistance of kinetochore fibers against anoxia-induced depolymerization is illustrated with representative metaphase figures (C). Bar, 5 μm. Moreover, inter-sister kinetochore distances were measured (n=125 sister kinetochore pairs from at least 18 different embryos) and the average (in μm ± s.d.) in prophase (pro) or metaphase (meta) is given in D. The average distance in normoxic (+O_2) and anoxic (–O_2) metaphase was found to be distinct (P<0.0001 in t-test; n=125). We did not detect significant variation in the average sister kinetochore separation with developmental stage (mitosis 11-13).

might be affected by anoxia. To characterize centrosome behavior in response to anoxia in further detail, we examined the centrosome components Aurora A, γ-tubulin, Centrosomin (Cnn) and D-TACC. Anoxia had only a subtle effect on Aurora A and γ-tubulin (Fig. 3A). In the resulting mitotic arrest the centrosomal pool of Aurora A and γ-tubulin had a more doughnut-shaped distribution with sharp outer borders, whereas in normoxic metaphase signals declined more gradually from the centrosome center towards the periphery (Fig. 3A, compare insets). Localization differences between anoxic and normoxic metaphases were similar but more pronounced in the case of Cnn (Fig. 3B). The characteristic flares of Cnn, which represent transport away and back to the centrosome primarily on dynamic astral microtubules (Megraw et al., 2002), were absent in anoxia. Cnn flaring on astral microtubules is known to be more extensive in interphase compared with metaphase (Megraw et al., 2002). Accordingly, the anoxia-induced elimination of Cnn flares was even more striking in interphase embryos (Fig. 3C). D-TACC localization

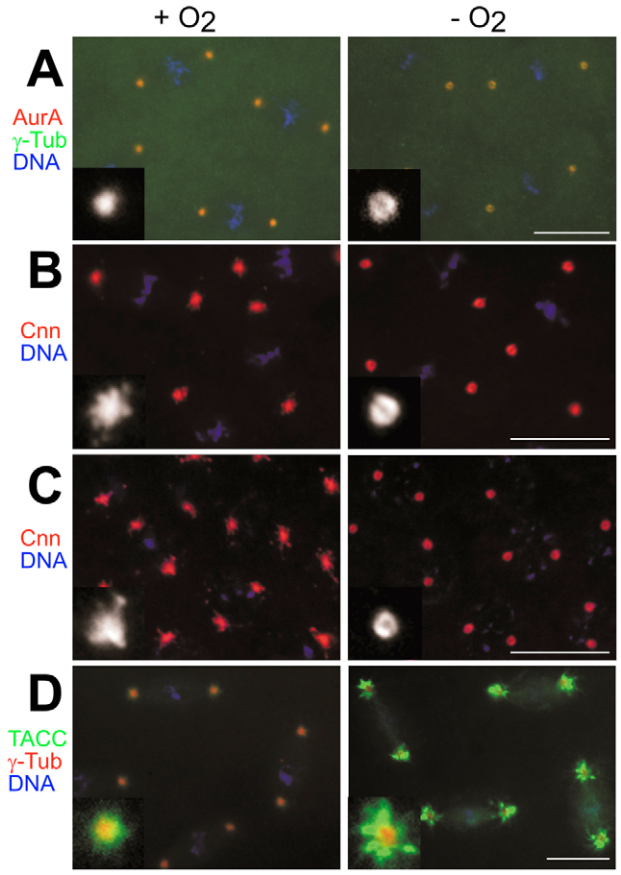

Fig. 3. Centrosome structure in anoxia. Syncytial blastoderm embryos were incubated (20 minutes) in either normoxic ($+O_2$) or anoxic ($-O_2$) buffer before fixation and immunolabeling. (A) Anti-Aurora A kinase (AurA), anti-γ-tubulin (γ-Tub) and DNA (DNA) during metaphase. (B) Anti-Centrosomin (Cnn) and DNA (DNA) during metaphase and (C) during interphase. (D) GFP-D-TACC (TACC), anti-γ-tubulin (γ-Tub) and DNA (DNA) during metaphase. Insets in the lower-left corners show a representative centrosome at higher magnification after labeling with anti-AurA (A) and anti-Cnn (B,C). Bars, 10 μm.

was also strongly affected by oxygen deprivation (Fig. 3D). However, D-TACC localization, which is known to stimulate astral microtubule plus-end growth (Barros et al., 2005; Kinoshita et al., 2005; Peset et al., 2005), was affected in a manner opposite to Aurora A, γ-tubulin and Cnn. D-TACC was found to be far less focused to centrosomes in anoxia (Fig. 3D). By in vivo imaging using embryos expressing GFP-D-TACC (data not shown), we analyzed the dynamics of D-TACC relocalization in response to oxygen deprivation. These analyses revealed that the striking D-TACC spikes were gradually built up after oxygen deprivation during prophase. At the time when anaphase onset would have occurred in normoxic conditions, D-TACC redistribution was subtle at most. During recovery from anoxia, GFP-D-TACC spikes were compacted back into the normal distribution within the period in which centrosome fiber regrowth was apparent in the GFP-α-tubulin imaging experiments (Fig. 1C). D-TACC function at the centrosome has been shown to be regulated by Aurora A, which phosphorylates an identified site on D-TACC (Barros et al., 2005). An antibody against this phosphoepitope (Barros et al., 2005) resulted in signal intensities that were not clearly altered by oxygen deprivation (data not shown), suggesting that Aurora A kinase activity is not inhibited, at least during the initial minutes of anoxia.

Similar effects on spindle organization as those triggered by anoxia have been observed in Schneider cells after knockdown of the kinesin family member Kin-8 (Klp67A) or dynein heavy chain 64C, whereas knockdown of many other components of the mitotic apparatus resulted in additional, structurally different spindle responses (Goshima et al., 2005). Therefore, we analyzed whether oxygen deprivation affects the localization of these motor proteins. Both motor proteins appeared to be rapidly and strongly affected. Oxygen deprivation induced a rapid reduction of Kin-8 levels within the spindle midzone already within 2 minutes (Fig. 4A). After 5 minutes of anoxia, Kin-8 spindle association was almost undetectable (Fig. 4A). With an antibody recognizing the *Drosophila* dynein light intermediate chain (D-LIC), we followed the response of dynein to anoxia. In normoxic metaphase, D-LIC was predominantly associated with the pseudo-cleavage furrows (Fig. 4B), as previously reported for dynein heavy chain (Cytrynbaum et al., 2005; Sharp et al., 2000a). After oxygen deprivation, D-LIC accumulated within minutes on spindle fibers in the vicinity of the kinetochores (Fig. 4B). The same behavior in response to anoxia was also observed by in vivo imaging embryos expressing a functional D-LIC version fused to GFP (data not shown). In these experiments, we also observed D-LIC-GFP particle movement on spindle fibers towards the pole (see below), suggesting that the dynein motor activity is not eliminated, at least during the initial minutes of anoxia.

Outer and constitutive inner kinetochore plate proteins are relocalized in response to anoxia

Kin-8 and dynein, which are rapidly affected by anoxia, are thought to provide important functions at the kinetochore (Savoian et al., 2004; Sharp et al., 2000b). Therefore, we characterized the response of centromere kinetochore complex components to oxygen deprivation. We did not observe rapid effects on the behavior of Cenp-A/Cid, a centromeric histone H3 variant that acts at the top of the centromere kinetochore

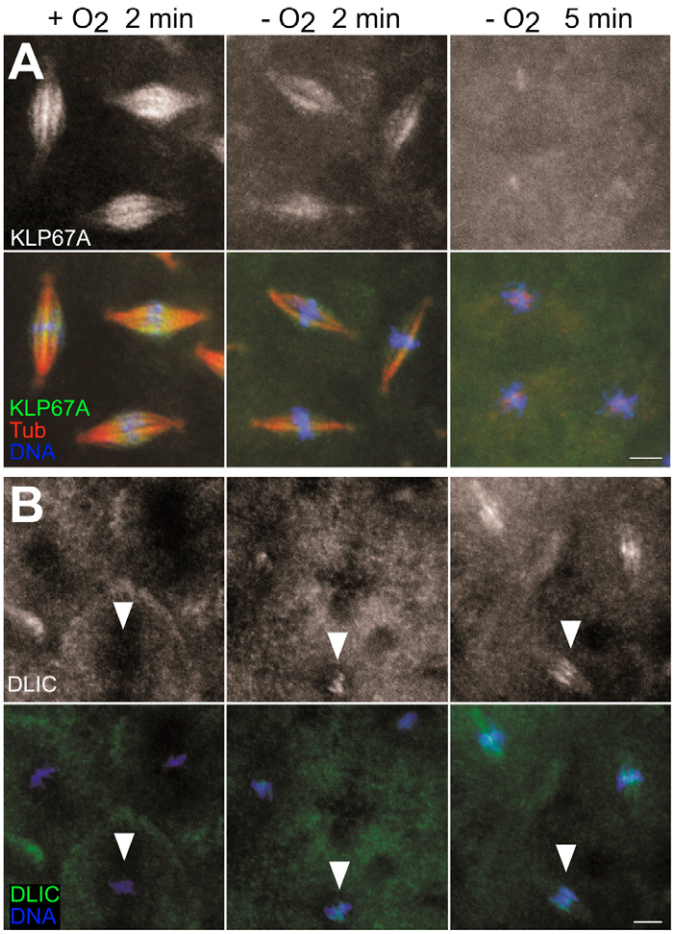

Fig. 4. Motor proteins in anoxia. Syncytial blastoderm embryos were incubated in either normoxic ($+O_2$) or anoxic ($-O_2$) buffer for 2 or 5 minutes before fixation and immunolabeling. (A) Anti-Kinesin 8/Klp67A (KLP67A), anti-α-tubulin (Tub) and DNA stain (DNA). Klp67A decreases rapidly in the central spindle region in response to anoxia. (B) Dynein light intermediate chain-GFP (DLIC) and DNA. Dynein accumulates rapidly at metaphase plates (arrowhead) in response to anoxia. Bars, 10 μm.

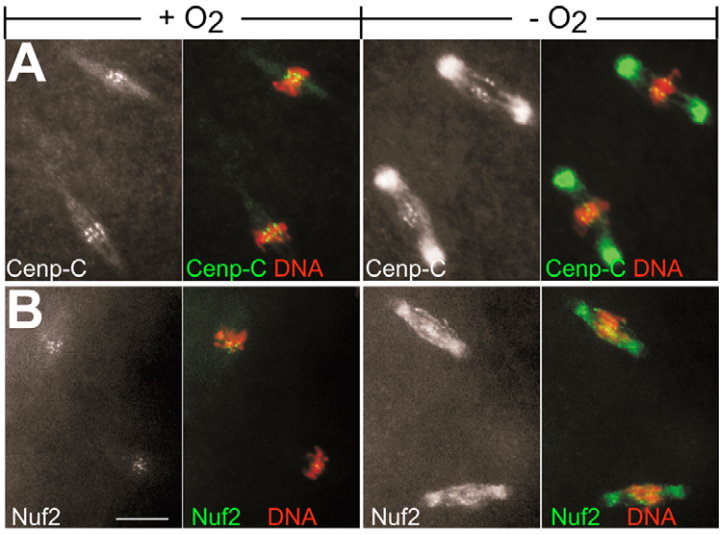

assembly process (Fig. 2C). Surprisingly, however, the localization of Cenp-C, another constitutive centromere protein of the inner kinetochore plate, was found to be severely affected by anoxia. An anoxia-induced redistribution of Cenp-C was observed by immunofluorescence after fixation (Fig. 5A), as well as by in vivo imaging (data not shown) of a functional enhanced yellow fluorescent protein (EYFP)-Cenp-C variant (Heeger et al., 2005). Cenp-C immunolabeling with two different affinity-purified rabbit antibodies indicated that a fraction of Cenp-C is spindle-associated even in normoxic syncytial embryos (Fig. 5A, and data not shown). In anoxic embryos, this Cenp-C pool appeared to be increased and redistributed to the centrosome-proximal spindle region (Fig. 5A). When anoxia was induced in the presence of the microtubule inhibitor colcemid (data not shown), EYFP-Cenp-C was found to be enriched on kinetochores, similar to that described for spindle checkpoint proteins (Hoffman et al., 2001). EYFP-Cenp-C accumulation in the vicinity of centrosomes was no longer observed under these conditions. Interestingly, we observed a similar anoxia-induced redistribution predominantly to the centrosome-proximal spindle region also for the outer kinetochore plate Ndc80/Hec1 complex component Nuf2 when analyzing the localization of a functional *Drosophila* EGFP-Nuf2 version (Fig. 5B). Therefore, we conclude that oxygen deprivation results in a redistribution of important kinetochore proteins. Nuf2 has a microtubule-binding activity (Cheeseman et al., 2006) and might form higher-order complexes with Cenp-C. It is possible, therefore, that the observed relocalization of these kinetochore proteins reflects anoxia effects on microtubules.

Kinetochore attachment to spindle fibers is thought to be regulated by the chromosomal passenger complex that includes Aurora B kinase and inner centromere protein (INCENP) (Vader et al., 2006). Using antibodies against *Drosophila* INCENP (Adams et al., 2001), we were unable to detect an extensive relocalization after anoxia induction during mitosis comparable to that observed for Cenp-C and Nuf2 (data not shown).

The response of spindle checkpoint proteins to anoxia

Because anoxia has rapid effects on the mitotic apparatus, we analyzed the response of mitotic spindle checkpoint proteins. Oxygen was deprived from embryos expressing functional EGFP fusion proteins and their localization was analyzed by in vivo imaging as well as after fixation. During normoxic metaphase some EGFP-Mps1 has been shown to be enriched on centrosomes and spindles and only weakly on kinetochores (Fischer et al., 2004). Apart from these localized signals, diffuse specific signals are observed as well (Fischer et al., 2004). In response to

Fig. 5. Kinetochore proteins in anoxia. Syncytial blastoderm embryos were incubated in either normoxic ($+O_2$) or anoxic ($-O_2$) buffer for 20 minutes before fixation and immunolabeling. (A) Anti-Cenp-C (Cenp-C) and DNA stain (DNA). (B) EGFP-Nuf2 (Nuf2) and DNA stain (DNA) in *gEGFP-Nuf2* embryos. In response to anoxia, Cenp-C and EGFP-Nuf2 accumulate on spindles predominantly in the centrosome-proximal region. Bar, 10 μm.

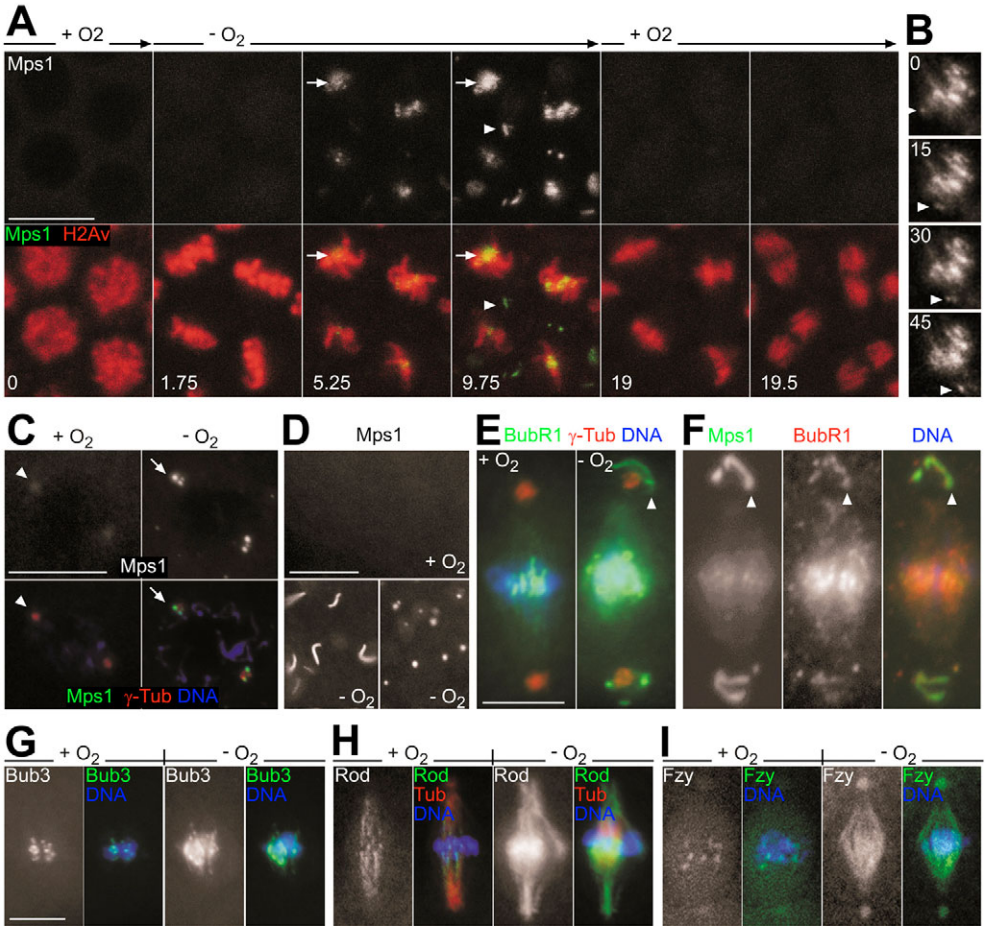

Fig. 6. Spindle checkpoint proteins in anoxia. (A) Selected frames after in vivo imaging of an embryo expressing EGFP-Mps1 (Mps1) and histone H2Av-mRFP (H2Av). Time in minutes is indicated in the frames showing the merged images in the bottom panel. Anoxia ($-O_2$) was induced at t=1.75 minutes after the onset of chromosome condensation during entry into mitosis. The resulting EGFP-Mps1 accumulation within the spindle midzone region of metaphase figures (arrows) and in centrosome-associated filaments (arrowheads) is indicated. The embryo was reoxygenated ($+O_2$) at t=9.75 minutes during the metaphase arrest, resulting in EGFP-Mps1 disappearance and completion of mitosis. Bar, 10 μm. (B) Frames showing EGFP-Mps1 at high magnification within the midzone region of a metaphase figure during the anoxia-induced mitotic arrest. Time in seconds is indicated within each frame. An EGFP-Mps1 particle moving along the spindle is indicated by arrowheads. (C) High-magnification views of single nuclei from syncytial *gEGFP-Mps1* embryos during interphase. The embryos were fixed and labeled with anti-γ-tubulin (γ-Tub) and DNA stain (DNA) after a 20-minute incubation in either normoxic ($+O_2$) or anoxic ($-O_2$) buffer. The weak centrosomal EGFP-Mps1 (Mps1) signals in normoxic embryos (arrowhead), as well as the strong signals in subcentrosomal dots in anoxic embryos (arrow), are indicated. Bar, 10 μm. (D) EGFP-Mps1 signals (Mps1) in cortical regions of preblastoderm embryos that were fixed after a 20-minute incubation in either normoxic ($+O_2$) or anoxic ($-O_2$) buffer. Anoxia induced filamentous or dot-like EGFP-Mps1 aggregates. Bar, 5 μm. (E) *gEGFP-BubR1* embryos were fixed and labeled with anti-γ-tubulin (γ-Tub) and DNA stain (DNA) after a 20-minute incubation in either normoxic ($+O_2$) or anoxic ($-O_2$) buffer. In response to anoxia, EGFP-BubR1 (BubR1) accumulates within the midzone region of metaphase figures and in peri-centrosomal filaments (arrowhead). Bar, 5 μm. (F) *gEGFP-Mps1* embryos were fixed and labeled with anti-BubR1 (BubR1) and DNA stain (DNA) after a 20-minute incubation in anoxic ($-O_2$) buffer. EGFP-Mps1 (Mps1) and anti-BubR1 signals largely overlap in the in peri-centrosomal filaments (arrowhead). (G,H,I) *gEGFP-Bub3* (G), *EGFP-Rod* (H) or *EGFP-Fzy* (I) embryos were fixed after a 20-minute incubation in either normoxic ($+O_2$) or anoxic ($-O_2$) buffer and labeled with a DNA stain (G-I; DNA) and anti-α-tubulin (H; Tub). Bar, 5 μm.

oxygen deprivation, EGFP-Mps1 strongly accumulated at kinetochores and was even more pronounced in the spindle fiber overlap zone in the equatorial plane (Fig. 6A, arrows). Interestingly, in approximately 5% of the embryos, impressive filamentous EGFP-Mps1 structures formed in the vicinity of the centrosomes in addition to the accumulation in the spindle midzone region (Fig. 6A, arrowheads). EGFP-Mps1 relocalization started within minutes after oxygen deprivation and reached a maximum after approximately 8 minutes. Recovery from anoxia (Fig. 6A) was accompanied by a return to the normal metaphase distribution before anaphase onset. We point out that the comparatively weaker signals of kinetochore- and spindle-associated EGFP-Mps1 before oxygen deprivation, as well as after reoxygenation, were not detectable with the confocal microscope settings adjusted for detection of the drastic EGFP-Mps1 enrichment within the midzone region during anoxia, as apparent in Fig. 6A.

Although the EGFP-Mps1 filaments close to centrosomes were only formed in some of the anoxic metaphase embryos, we observed EGFP-Mps1 aggregation far more frequently in the cortical region of anoxic preblastoderm embryos in which nuclei have not yet migrated out to the egg periphery. EGFP-Mps1 aggregation occurred in approximately 80% of the anoxic preblastoderm embryos, usually in the form of bright dots but occasionally also in filamentous structures (Fig. 6D).

EGFP-BubR1 behavior in response to anoxia was very similar to EGFP-Mps1. In mitotic cells, enrichment also occurred within the spindle midzone region (Fig. 6E), although less pronounced than with EGFP-Mps1. After oxygen deprivation, we also observed EGFP-BubR1 aggregation within the cortical region of preblastoderm embryos (data not shown), as well as filament formation around centrosomes in syncytial blastoderm embryos during mitosis (Fig. 6E), at comparable frequencies as with EGFP-Mps1. Double labeling

indicated colocalization of BubR1 and EGFP-Mps1 within these aggregates (Fig. 6F). Colocalization was not perfect, however, perhaps reflecting antibody accessibility problems.

To analyze the behavior of *Drosophila* Bub3 in response to anoxia, we established a *gEGFP-Bub3* transgene that was found to rescue the recessive lethality associated with a newly identified *Bub3* mutation. Similar to EGFP-Mps1 and EGFP-BubR1, we also observed an enrichment of EGFP-Bub3 within the spindle midzone region in response to oxygen deprivation (Fig. 6G). However, EGFP-Bub3 was never observed in aggregated dots within the cortical region or in filaments around the centrosomal region in anoxic embryos.

In metazoans, the RZZ complex that includes the Rod protein has been implicated in the mitotic spindle checkpoint and shown to recruit the Mad2 checkpoint protein to kinetochores and spindle fibers (Buffin et al., 2005; Karess, 2005). In response to anoxia, EGFP-Rod was strongly enriched on metaphase spindles, in particular within the spindle midzone region (Fig. 6H). As expected, the behavior of EGFP-Mad2 in response to anoxia was highly similar to EGFP-Rod (data not shown). The RZZ complex is also known to interact with the dynein/dynactin motor protein complex that mediates the shedding of Mad2 and presumably other spindle checkpoint proteins away from bioriented kinetochores along kinetochore fibers. As observed in normoxic larval neuroblasts (Basto et al., 2004), dynein behavior (Fig. 4B) appeared to be similar but not identical to the RZZ complex and Mad2 in anoxic embryos. Interestingly, with D-LIC-GFP and EGFP-Rod (data not shown), as well as with EGFP-Mps1 (Fig. 6B), we observed particle transport along spindle fibers during the anoxia-induced metaphase arrest, suggesting that dynein motor activity is not abolished by anoxia, at least initially.

Spindle checkpoint activation results in Fzy/Cdc20 inhibition through Mad2 and BubR1. This inhibition prevents the anaphase-promoting complex or cyclosome (APC/C)-mediated degradation of securin and B-type cyclins and thereby anaphase onset. Consistent with the proposed complex formation between Fzy and activated Mad2 and BubR1, anoxia was found to result in an enrichment of EGFP-Fzy on metaphase spindles (Fig. 6I), similar to the other analyzed mitotic spindle checkpoint components. In addition, EGFP-Fzy was also found on centrosomes in anoxic metaphase embryos.

Interestingly, some spindle checkpoint components were not only redistributed during mitosis in response to oxygen deprivation, but also during interphase. In normoxic interphase embryos, EGFP-Mps1 is very weakly enriched on centrosomes (Fig. 6C) (Fischer et al., 2004). After oxygen deprivation, EGFP-Mps1 was observed in very bright and highly focused spots (Fig. 6C) that were closely associated with interphase centrosomes and which possibly represent centriolar structures. The same behavior was also observed with EGFP-BubR1 (data not shown). Similarly, EGFP-Bub3 enrichment on centrosomes was not detected in normoxic but strongly in anoxic interphase embryos (data not shown).

The observed relocalization of EGFP-Mps1 and EGFP-Bub3 in anoxic interphase embryos raised the possibility that oxygen deprivation activates the spindle checkpoint not only during mitosis but also during interphase. Spindle checkpoint activation in various experimental systems is correlated with an electrophoretic mobility shift of several components (Chen, 2002; Chen, 2004; Hardwick and Murray, 1995; Stucke et al., 2002), including *Drosophila* Mps1 (Fig. 7 and data not shown). Therefore, we analyzed whether oxygen deprivation during interphase leads to an Mps1 mobility shift. However, we did not detect such a shift, even though it was clearly observed during prometaphase of normal mitosis and in the anoxic metaphase arrest (Fig. 7).

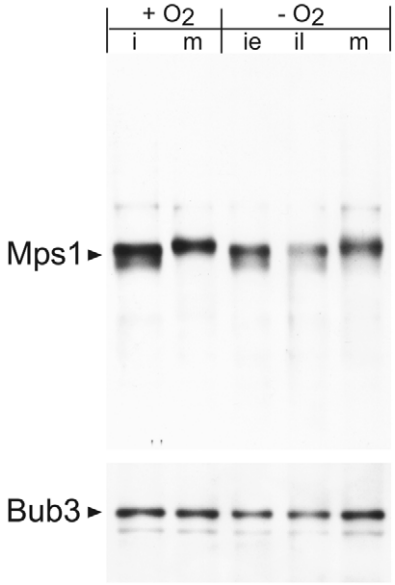

Fig. 7. Mps1 modification in response to anoxia. *gEGFP-Bub3* embryos were fixed and labeled with DNA stain (DNA) after a 20-minute incubation in either normoxic ($+O_2$) or anoxic ($-O_2$) buffer. Syncytial blastoderm embryos during interphase (i) or metaphase (m) were sorted using a microscope. Anoxic interphase embryos were further sorted into early interphase (ie) and late interphase (il) based on the appearance of chromatin that is condensed into a meshwork during early interphase and into distinct chromatids during late interphase. Sorted embryos were used for extract preparation and immunoblotting with anti-Mps1 (Mps1) and anti-GFP (Bub3).

From our characterization of spindle checkpoint components (Mps1, BubR1, Bub3, Rod, Mad2) and the final target (Fzy), we conclude that anoxia rapidly affects their behavior (even during interphase in the case of Mps1 and Bub3) and activates the checkpoint pathway during mitosis.

Comparison of the consequences of anoxia and metabolic inhibitors

The drop in ATP levels after oxygen deprivation has been shown to be less than 10% within the time sufficient to induce a metaphase arrest (DiGregorio et al., 2001). This modest drop is not expected to have pronounced effects on protein kinase and motor protein activities based on biochemical analyses in vitro in which Km values for ATP are usually found to be within the μM range, contrasting with mM ATP concentrations in vivo. Our findings described above strongly support the notion that kinases and motors retain at least some activity after oxygen deprivation within the first minutes. Mitotic spindle checkpoint activation involves protein kinase activities (Mps1, BubR1) and it occurs in response to oxygen deprivation despite apparently ongoing dynein/dynactin-mediated transport along spindle fibers. Similarly, motor activity of the *Drosophila* kinesin-14 Ncd has recently been described in oxygen-

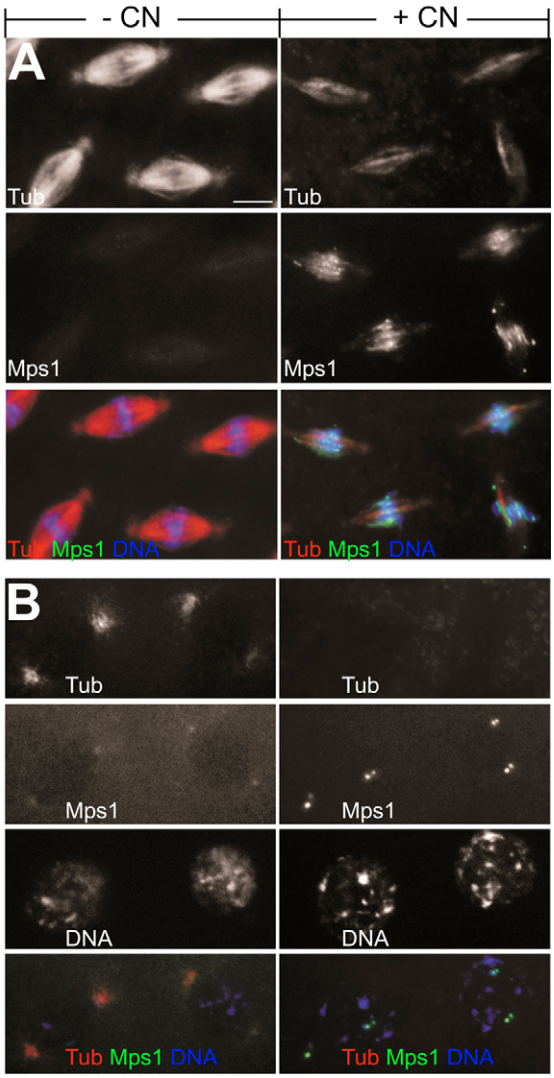

Fig. 8. Spindle checkpoint activation by cytochrome oxidase inhibitor. *gEGFP-Mps1* embryos were incubated in either absence (–CN) or presence (+CN) of cyanide for 5 (A) or 15 (B) minutes before fixation and labeling with anti-α-tubulin (Tub) and a DNA stain (DNA). Cyanide induces reorganization of EGFP-Mps1 (Mps1), microtubules and chromatin during metaphase (A) and interphase (B) that is indistinguishable from the effects of anoxia. Bar, 5 μm.

deprived embryos (Sciambi et al., 2005). It is conceivable, therefore, that anoxia might activate the mitotic spindle checkpoint independent of its effect on oxidative phosphorylation and ATP levels. Accordingly, inhibition of oxidative phosphorylation in the presence of oxygen would not be expected to result in spindle checkpoint activation. To address whether inhibition of oxidative phosphorylation in the presence of oxygen results in spindle checkpoint activation, we incubated syncytial embryos in medium containing azide (data not shown) or cyanide (Fig. 8). These cytochrome oxidase inhibitors were observed to have rapid effects on metaphase spindle organization and EGFP-Mps1 localization (Fig. 8A). Moreover, the effects appeared to be indistinguishable from those induced by oxygen deprivation. In addition, the metabolic inhibitors also mimicked the effects of oxygen deprivation on chromatin condensation and centrosomal EGFP-Mps1 during interphase (Fig. 8B). Therefore, we conclude that spindle checkpoint activation by anoxia is presumably caused by inhibition of oxidative phosphorylation.

Discussion

Anoxia effects on spindle organization have been reported previously (Douglas et al., 2001; Hajeri et al., 2005; Sciambi et al., 2005). However, the spindle abnormalities described in earlier studies were observed after prolonged exposure to anoxia for more than 10 minutes. Therefore, these studies did not rule out the possibility that the observed spindle abnormalities result secondarily as a consequence of spindle checkpoint activation. By contrast, our analyses in checkpoint-deficient *Mps1* mutant embryos demonstrate that the spindle abnormalities are not simply the consequence of the anoxia-induced mitotic arrest. Moreover, we demonstrate that anoxia effects on the mitotic spindle are so rapid that spindle defects can be the cause of the observed mitotic arrest. To cause a mitotic arrest during the rapid syncytial cycles, anoxia has to be induced after entry into mitosis (otherwise it leads to an interphase arrest) and the consequences must be sensed in the embryo before the onset of anaphase, which occurs only 4.5 minutes after entry into mitosis (Minden et al., 1989). Our analyses have revealed spindle abnormalities already 2 minutes after anoxia induction during early mitosis.

The spindle abnormalities that develop within minutes after oxygen deprivation are accompanied by a reduced separation of sister kinetochores in metaphase plates. The inter-kinetochore distance in metaphase is thought to reflect the pulling forces exerted by the spindle on bioriented chromosomes. Accordingly, anoxia appears to reduce these pulling forces. In principle, the observed decrease in the inter-kinetochore distance might also reflect reduced chromosome elasticity. Because oxygen deprivation induces chromatin condensation at least in interphase (Foe and Alberts, 1985), increased stiffness of anoxic metaphase chromosomes should not be discounted prematurely. Nevertheless, our observation in the checkpoint-deficient *Mps1* mutant embryos that the speed of chromosome congression in prometaphase and of chromosome segregation to the poles in anaphase is markedly slower in anoxia compared with normoxia, is also consistent with the notion of reduced spindle forces acting on chromosomes in anoxia.

The rapid effects of oxygen deprivation on spindles and chromosome attachment can therefore readily explain why mitotic spindle checkpoint activity is maintained in anoxia. All the mitotic spindle checkpoint proteins analyzed (Mps1, BubR1, Bub3, Rod, Mad2) as well as their target Fzy/Cdc20 accumulate strongly on anoxic spindles, predominantly in the spindle midzone region. A similar accumulation has been observed in normoxic embryos in response to taxol in experiments with EGFP-BubR1, EGRFP-Rod and EGFP-Mad2 (Buffin et al., 2005). Moreover, Mps1 has a low electrophoretic mobility in anoxic metaphase extracts, as also observed in normoxic metaphase and in colchicine arrest (data not shown). Interestingly, some mitotic spindle checkpoint proteins (Mps1 and Bub3) were also observed to relocalize in interphase in response to anoxia. However, based on the Mps1 behavior revealed in our immunoblotting experiments, anoxia

does not appear to activate the mitotic spindle checkpoint during interphase. This further argues against a physiological link that would allow mitotic spindle checkpoint activation by anoxia independent of effects on the mitotic apparatus.

The anoxia response of Mps1 and Bub3 during interphase might also reflect altered microtubule dynamics. The same interphase response was also induced by the inhibitors of oxidative phosphorylation, KCN and NaN_3. A rapid reduction of microtubule asters induced by these various treatments therefore occurs during both mitosis and interphase. Aster reduction might reflect increased microtubule instability or reduced centrosomal nucleation activity. The centrosomal components Cnn and TACC are clearly reorganized after anoxia induction during interphase, whereas other components (γ-tubulin and Aurora A) were only subtly affected. Moreover, the Cnn-containing flares of pericentrosomal material, which are moved by microtubule dynamics independent of motors during normoxia (Megraw et al., 2002), are eliminated by anoxia. We note that an opposite response of aster microtubules has been observed with mitotic mammalian cells in culture after treatment with cyanide and 2-deoxyglucose (Wadsworth and Salmon, 1988). These conditions are expected to induce a more drastic reduction in ATP levels because they inhibit glycolysis in addition to oxidative phosphorylation.

In addition to centrosomal proteins, anoxia affects the localization of spindle-associated protein Kin-8/KLP67A and dynein. Our observations are in accord with those of others (Howell et al., 2001; Sciambi et al., 2005) and argue against the possibility that the rapid effects on these proteins reflect an inhibition of their motor activity. Similarly, our observations argue that the activity of protein kinases (such as Mps1, BubR1 and Aurora A) is not inhibited during the initial response to anoxia. We would like to speculate, therefore, that microtubule dynamics might be highly sensitive to oxygen deprivation, being affected well before a general inhibition of motor proteins and kinase activities occurs. Accordingly, the observed anoxia-induced relocalization of all the proteins analyzed in our studies, including the kinetochore proteins Cenp-C and Nuf2, might reflect altered microtubule dynamics. However, the rapid chromatin condensation that is induced by anoxia during interphase (Foe and Alberts, 1985) is very unlikely to be linked to microtubule dynamics, indicating the existence of sensitive anoxia targets other than microtubules.

Our finding that metabolic inhibitors (CN^-, N_3^-) and anoxia have indistinguishable early effects is consistent with the notion that minor reductions of ATP levels might cause the observed effects. We also point out that the recovery dynamics of ATP levels after reoxygenation was found to be closely correlated to resumption of mitosis (DiGregorio et al., 2001). Because the highly abundant cellular component tubulin is directly regulated by guanosine triphosphate (GTP), which in turn is generated from ATP, it is conceivable that microtubule dynamics respond immediately to changes in ATP levels. However, we point out that apart from effects on ATP levels, inhibition of oxidative phosphorylation is known to have many other consequences such as a collapse of mitochondrial potential and increases in NADH, ADP and reactive oxygen species. Additional analysis will certainly be required for the identification of the sensitive targets of anoxia and the molecular details of their response.

In summary, anoxia in combination with spindle checkpoint defects drastically enhances chromosome instability in *C. elegans* and *D. melanogaster* and possibly during cancer development in humans as well. Our analyses with syncytial *D. melanogaster* embryos provide insights into the mechanism of spindle checkpoint activation by anoxia. Oxygen deprivation and inhibitors of oxidative phosphorylation were shown to affect microtubule organization within minutes and independent of spindle checkpoint function. Kinetochore attachment to the spindle and chromosome segregation during mitosis are far more readily impaired by oxygen depletion than spindle checkpoint activation. As a consequence, spindle checkpoint activation in response to acute anoxia can provide protection from aneuploidies.

Materials and Methods

Fly stocks

The following fly strains have been described before: *Mps1*^{1} and *P{gEGFP-Mps1}* (Fischer et al., 2004), *P{gcid-EGFP-cid}*, *P{gEYFP-Cenp-C}* and *P{His2Av-mRFP1}* (Heeger et al., 2005), *P{gEGFP-Nuf2}* (Schittenhelm et al., 2007), *w*^{1118}; *P{w*$^{+mC}$*=GAL4::VP16-nos.UTR}MVD1*, *P{w*$^{+mC}$*=UASp-GFPS65C-alphaTub84B}3* (Grieder et al., 2000), *G147* (Morin et al., 2001), *P{gEGFP-Rod}*, *P{gEGFP-BubR1}* and *P{gEGFP-Mad2}* (Buffin et al., 2005), *P{Ubi-EGFP-Fzy}* (Raff et al., 2002) and *P{Ubi-TACC-GFP}* (Barros et al., 2005). *P{Ubi-DLIC-GFP}* was kindly provided by Jordan Raff (Department of Genetics, The Wellcome/CRC Institute, Cambridge, UK) before publication. We used *w*^{1} for control experiments because all the analyzed mutations and transgenes were in a *w* mutant background. Females with *Mps1*^{1} germ-line clones were generated using the flippase (FLP)-dominant female sterility (DFS) technique (Chou and Perrimon, 1996) as described previously (Fischer et al., 2004), and the term *Mps1* mutant embryos refers to the progeny derived from these females.

P{gEGFP-Bub3} lines were obtained by standard germ-line transformation using a pP{CaSpeR-4} construct. For its construction, we amplified the genomic *Bub3* region from BAC RPC1-98 10L12 (Hoskins et al., 2000) using the primers RaS7 (5′-GATGAATTCAGGGGAAGGACGAACTGG-3′) and RaS8 (5′-ACGATCTA-GAATGCTTGGGCAACAATTCCGA-3′), which introduced an *Eco*RI and an *Xba*I site, respectively. After digestion with *Eco*RI and *Xba*I, the amplification product was inserted into the corresponding sites of pP{CaSpeR-4} to generate *P{gBub3}* lines. To insert the EGFP coding sequence just before the initiation codon, we subcloned an *Eco*RI-*Bgl*II fragment from the *P{gBub3}* construct into pLitmus28Δ*Eco*RV-*Stu*I. Into the resulting cloning intermediate, we introduced restriction sites for *Bam*HI, *Sma*I and *Not*I immediately upstream of the *Bub3* initiation codon by inverse PCR using the primers RP23 (5′-TGGGCCCGG-GATCCTGTCAAGTTTTCTGCTAGCA-3′) and RP24 (5′-GCAGCCCGGGCG-GCCGCATGCGTCCCCCAGAGTTCAA-3′). The *Bam*HI-*Not*I fragment including the *Sma*I site was subsequently replaced with a *Bam*HI-*Not*I fragment containing the complete EGFP coding sequence. Finally, the recombinant *Eco*RI-*Bgl*II fragment with the EGFP sequence was used to replace the corresponding region in *P{gBub3}*. After sequence confirmation, several independent *P{gBub3}* and *P{gEGFP-Bub3}* lines were established. Complementation tests using *Bub3*^{233} mutant flies indicated that both transgenes, *P{gBub3}* and *P{gEGFP-Bub3}*, were functional. *Bub3*^{233} carries a *pBac{tTA}* mutator element (Horn et al., 2003) within the 5′ untranslated region (UTR) of *Bub3*, resulting in recessive lethality at the larval/pupal interphase. *Bub3*^{233} homozygotes carrying *P{gBub3}* or *P{gEGFP-Bub3}* were found to be fully viable and fertile.

In vivo imaging

Embryos were aged to the syncytial blastoderm stages after collection on apple juice agar plates. Dechorionated embryos were lined up, immobilized on coverslips and covered with halocarbon oil. Time-lapse confocal laser-scanning microscopy was performed with a Leica TCS SP1 system in combination with an inverted microscope at 22-24°C in a temperature-controlled room. To avoid light damage, excitation laser intensity was minimized and the pinhole was opened. In most experiments, two frames (1024×1024 pixels) were acquired and averaged, at 15-second intervals using a 63× glycerol immersion objective, sometimes in combination with fourfold electronic zoom magnification.

For induction of anoxia, we covered the embryos mounted under halocarbon oil on the glass coverslip with a glass cylinder (20 mm diameter, 30 mm high), which was closed on one side except for two small openings (2 mm diameter), using silicon grease for air-tight sealing. Air in the glass cylinder was then displaced by applying a flow of nitrogen, argon or carbon dioxide gas through silicon tubing connected to one of the top openings and to a gas container on the other end. Reoxygenation was achieved by stopping the gas flow. The presented findings were observed in several independent experiments for each genotype and physiological condition.

Immunofluorescence

Embryos were collected and aged to the appropriate developmental stage before chorion removal. To induce anoxia, half of the embryos were subsequently incubated in extensively degassed 0.7% NaCl and 0.07% Triton-X-100 (NaCl-TX) for 2 to 20 minutes. The other half of the embryos were incubated at the same time in normal NaCl-TX for normoxic control experiments. For the inhibitor experiments, we incubated half of the dechorionated embryos in 4 mM KCN or 4 mM NaN_3 in phosphate-buffered saline (PBS) for 5 to 15 minutes. For control experiments, the other half of the embryos were incubated in 4 mM KCl in PBS for the same amount of time. Embryos were rapidly fixed and devitellinized after these incubations by replacing NaCl-TX or PBS with a 1:1 mixture of heptane and methanol. The concentration of the inhibitors of oxidative phosphorylation was chosen because 4 mM of NaCN has previously been shown to reduce ATP levels with comparable kinetics as oxygen deprivation (DiGregorio et al., 2001).

For immunofluorescent staining we used mouse monoclonal antibody DM1A anti-α-tubulin (Sigma) at 1:8000, affinity-purified rabbit anti-Cenp-A/Cid (Jäger et al., 2005) at 1:1000, affinity-purified rabbit anti-Cenp-C (Heeger et al., 2005) at 1:5000, rabbit anti-BubR1 (kindly provided by C. Sunkel, Universidade do Porto, Portugal) at 1:2000, rabbit anti-INCENP (Adams et al., 2001) at 1:500, rabbit anti-KLP67A (Savoian et al., 2004) at 1:50, mouse monoclonal 74.1 anti-dynein intermediate chain (Dillman, 3rd and Pfister, 1994) (Abcam) at 1:300, rabbit anti-Aurora A (Barros et al., 2005) at 1:250, rabbit anti-phospho-TACC (Barros et al., 2005) at 1:500, rabbit anti-Centrosomin (Heuer et al., 1995) at 1:200, and mouse monoclonal GTU-88 anti-γ-tubulin (Sigma) at 1:500. DNA was labeled with 1 μg/ml Hoechst 33258. Single focal planes or z-stacks were acquired with a Zeiss Axioplan 2 Imaging system using Zeiss AxioVision software. For comparison of stained anoxic and normoxic wild-type embryos, the first 20 randomly chosen embryos in metaphase were imaged. Galleries were compared and used for the selection of representative embryos. Moreover, at least two additional independent experiments were used to confirm the reproducibility of the findings. Adobe Photoshop was used for preparation of the figures.

Immunoblotting

Embryos were collected and aged to the syncytial blastoderm stage before chorion removal. Samples of embryos were incubated in either NaCl-TX or Schneider's *Drosophila* cell culture medium containing 10 μM colcemid (N-Deacetyl-N-methylcolchicine, Sigma) or in extensively degassed NaCl-TX for 20 minutes. After methanol fixation and DNA staining, interphase or metaphase embryos were selected with the help of an inverted microscope and pooled before extract preparation (Edgar et al., 1994). Extracts were resolved by sodium dodecyl sulfate-polyacrylamide gel electrophoresis. For production of rabbit antibodies against *Drosophila* Mps1, we expressed an Mps1 fragment (amino acids 150-630) in *Escherichia coli* with an N-terminal His_6 extension. Ni-NTA chromatography was used for purification of the immunogen. Antibodies were affinity-purified after immobilization of the immunogen on CNBr-activated sepharose (Sigma). Immunoblots were probed with affinity-purified rabbit anti-Mps1 at 1:5000 and affinity-purified rabbit anti-EGFP (kindly provided by S. Heidmann, University of Bayreuth, Germany) at 1:3000 using Hybond-ECL membranes and ECL detection (Amersham Biosciences).

We thank F. Althoff, U. Großkinsky and R. Schittenhelm for providing reagents and help during initial experiments. We are also grateful to W. Earnshaw, D. Glover, R. Karess, T. Kaufman, J. Raff and C. Sunkel for antibodies and fly stocks. Moreover, we thank S. Heidmann for comments on the manuscript. This work was supported by the Deutsche Forschungsgemeinschaft (DFG LE 987/3-3, 3-4 and 4-1).

References

Adams, R. R., Maiato, H., Earnshaw, W. C. and Carmena, M. (2001). Essential roles of Drosophila inner centromere protein (INCENP) and aurora B in histone H3 phosphorylation, metaphase chromosome alignment, kinetochore disjunction, and chromosome segregation. *J. Cell Biol.* **153**, 865-880.

Barros, T. P., Kinoshita, K., Hyman, A. A. and Raff, J. W. (2005). Aurora A activates D-TACC-Msps complexes exclusively at centrosomes to stabilize centrosomal microtubules. *J. Cell Biol.* **170**, 1039-1046.

Basto, R., Scaerou, F., Mische, S., Wojcik, E., Lefebvre, C., Gomes, R., Hays, T. and Karess, R. (2004). In vivo dynamics of the rough deal checkpoint protein during Drosophila mitosis. *Curr. Biol.* **14**, 56-61.

Buffin, E., Lefebvre, C., Huang, J., Gagou, M. E. and Karess, R. E. (2005). Recruitment of Mad2 to the kinetochore requires the Rod/Zw10 complex. *Curr. Biol.* **15**, 856-861.

Cheeseman, I. M., Chappie, J. S., Wilson-Kubalek, E. M. and Desai, A. (2006). The conserved KMN network constitutes the core microtubule-binding site of the kinetochore. *Cell* **127**, 983-997.

Chen, R. H. (2002). BubR1 is essential for kinetochore localization of other spindle checkpoint proteins and its phosphorylation requires Mad1. *J. Cell Biol.* **158**, 487-496.

Chen, R. H. (2004). Phosphorylation and activation of Bub1 on unattached chromosomes facilitate the spindle checkpoint. *EMBO J.* **23**, 3113-3121.

Chou, T. B. and Perrimon, N. (1996). The autosomal FLP-DFS technique for generating germline mosaics in Drosophila melanogaster. *Genetics* **144**, 1673-1679.

Cytrynbaum, E. N., Sommi, P., Brust-Mascher, I., Scholey, J. M. and Mogilner, A. (2005). Early spindle assembly in Drosophila embryos: role of a force balance involving cytoskeletal dynamics and nuclear mechanics. *Mol. Biol. Cell* **16**, 4967-4981.

DiGregorio, P. J., Ubersax, J. A. and O'Farrell, P. H. (2001). Hypoxia and nitric oxide induce a rapid, reversible cell cycle arrest of the Drosophila syncytial divisions. *J. Biol. Chem.* **276**, 1930-1937.

Dillman, J. F., 3rd and Pfister, K. K. (1994). Differential phosphorylation in vivo of cytoplasmic dynein associated with anterogradely moving organelles. *J. Cell Biol.* **127**, 1671-1681.

Douglas, R. M., Xu, T. and Haddad, G. G. (2001). Cell cycle progression and cell division are sensitive to hypoxia in Drosophila melanogaster embryos. *Am. J. Physiol. Regul. Integr. Comp. Physiol.* **280**, R1555-R1563.

Douglas, R. M., Farahani, R., Morcillo, P., Kanaan, A., Xu, T. and Haddad, G. G. (2005). Hypoxia induces major effects on cell cycle kinetics and protein expression in Drosophila melanogaster embryos. *Am. J. Physiol. Regul. Integr. Comp. Physiol.* **288**, R511-R521.

Edgar, B. A., Lehman, D. A. and O'Farrell, P. H. (1994). Transcriptional regulation of string(cdc25): a link between developmental programming and the cell cycle. *Development* **120**, 3131-3143.

Fischer, M. G., Heeger, S., Hacker, U. and Lehner, C. F. (2004). The mitotic arrest in response to hypoxia and of polar bodies during early embryogenesis requires Drosophila Mps1. *Curr. Biol.* **14**, 2019-2024.

Foe, V. E. and Alberts, B. M. (1985). Reversible chromosome condensation induced in Drosophila embryos by anoxia: visualization of interphase nuclear organization. *J. Cell Biol.* **100**, 1623-1636.

Gorr, T. A., Gassmann, M. and Wappner, P. (2006). Sensing and responding to hypoxia via HIF in model invertebrates. *J. Insect Physiol.* **52**, 349-364.

Goshima, G., Wollman, R., Stuurman, N., Scholey, J. M. and Vale, R. D. (2005). Length control of the metaphase spindle. *Curr. Biol.* **15**, 1979-1988.

Grieder, N. C., de Cuevas, M. and Spradling, A. C. (2000). The fusome organizes the microtubule network during oocyte differentiation in Drosophila. *Development* **127**, 4253-4264.

Hajeri, V. A., Trejo, J. and Padilla, P. A. (2005). Characterization of sub-nuclear changes in Caenorhabditis elegans embryos exposed to brief, intermediate and long-term anoxia to analyze anoxia-induced cell cycle arrest. *BMC Cell Biol.* **6**, 47.

Hardwick, K. G. and Murray, A. W. (1995). Mad1p, a phosphoprotein component of the spindle assembly checkpoint in budding yeast. *J. Cell Biol.* **131**, 709-720.

Heeger, S., Leismann, O., Schittenhelm, R., Schraidt, O., Heidmann, S. and Lehner, C. F. (2005). Genetic interactions of Separase regulatory subunits reveal the diverged Drosophila Cenp-C homolog. *Genes Dev.* **19**, 2041-2053.

Heuer, J. G., Li, K. J. and Kaufman, T. C. (1995). The Drosophila homeotic target gene centrosomin (cnn) encodes a novel centrosomal protein with leucine zippers and maps to a genomic region required for midgut morphogenesis. *Development* **121**, 3861-3876.

Hockel, M. and Vaupel, P. (2001). Tumor hypoxia: definitions and current clinical, biologic, and molecular aspects. *J. Natl. Cancer Inst.* **93**, 266-276.

Hoffman, D. B., Pearson, C. G., Yen, T. J., Howell, B. J. and Salmon, E. D. (2001). Microtubule-dependent changes in assembly of microtubule motor proteins and mitotic spindle checkpoint proteins at PtK1 kinetochores. *Mol. Biol. Cell* **12**, 1995-2009.

Horn, C., Offen, N., Nystedt, S., Hacker, U. and Wimmer, E. A. (2003). piggyBac-based insertional mutagenesis and enhancer detection as a tool for functional insect genomics. *Genetics* **163**, 647-661.

Hoskins, R. A., Nelson, C. R., Berman, B. P., Laverty, T. R., George, R. A., Ciesiolka, L., Naeemuddin, M., Arenson, A. D., Durbin, J., David, R. G. et al. (2000). A BAC-based physical map of the major autosomes of Drosophila melanogaster. *Science* **287**, 2271-2274.

Howell, B. J., McEwen, B. F., Canman, J. C., Hoffman, D. B., Farrar, E. M., Rieder, C. L. and Salmon, E. D. (2001). Cytoplasmic dynein/dynactin drives kinetochore protein transport to the spindle poles and has a role in mitotic spindle checkpoint inactivation. *J. Cell Biol.* **155**, 1159-1172.

Jäger, H., Rauch, M. and Heidmann, S. (2005). The Drosophila melanogaster condensin subunit Cap-G interacts with the centromere-specific histone H3 variant CID. *Chromosoma* **113**, 350-361.

Jiang, H., Guo, R. and Powell-Coffman, J. A. (2001). The Caenorhabditis elegans hif-1 gene encodes a bHLH-PAS protein that is required for adaptation to hypoxia. *Proc. Natl. Acad. Sci. USA* **98**, 7916-7921.

Karess, R. (2005). Rod-Zw10-Zwilch: a key player in the spindle checkpoint. *Trends Cell Biol.* **15**, 386-392.

Kellogg, D. R., Mitchison, T. J. and Alberts, B. M. (1988). Behaviour of microtubules and actin filaments in living Drosophila embryos. *Development* **103**, 675-686.

Kinoshita, K., Noetzel, T. L., Pelletier, L., Mechtler, K., Drechsel, D. N., Schwager, A., Lee, M., Raff, J. W. and Hyman, A. A. (2005). Aurora A phosphorylation of TACC3/maskin is required for centrosome-dependent microtubule assembly in mitosis. *J. Cell Biol.* **170**, 1047-1055.

Kops, G. J., Weaver, B. A. and Cleveland, D. W. (2005). On the road to cancer: aneuploidy and the mitotic checkpoint. *Nat. Rev. Cancer* **5**, 773-785.

Lavista-Llanos, S., Centanin, L., Irisarri, M., Russo, D. M., Gleadle, J. M., Bocca, S. N., Muzzopappa, M., Ratcliffe, P. J. and Wappner, P. (2002). Control of the hypoxic response in Drosophila melanogaster by the basic helix-loop-helix PAS protein similar. *Mol. Cell. Biol.* **22**, 6842-6853.

Logarinho, E., Bousbaa, H., Dias, J. M., Lopes, C., Amorim, I., Antunes-Martins, A.

and Sunkel, C. E. (2004). Different spindle checkpoint proteins monitor microtubule attachment and tension at kinetochores in Drosophila cells. *J. Cell Sci.* **117**, 1757-1771.
McIntosh, J. R., Grishchuk, E. L. and West, R. R. (2002). Chromosome-microtubule interactions during mitosis. *Annu. Rev. Cell Dev. Biol.* **18**, 193-219.
Megraw, T. L., Kilaru, S., Turner, F. R. and Kaufman, T. C. (2002). The centrosome is a dynamic structure that ejects PCM flares. *J. Cell Sci.* **115**, 4707-4718.
Minden, J. S., Agard, J. W., Sedat, J. W. and Alberts, B. M. (1989). Direct cell lineage analysis in Drosophila melanogaster by time lapse three dimensional optical microscopy of living embryos. *J. Cell Biol.* **109**, 505-516.
Morin, X., Daneman, R., Zavortink, M. and Chia, W. (2001). A protein trap strategy to detect GFP-tagged proteins expressed from their endogenous loci in Drosophila. *Proc. Natl. Acad. Sci. USA* **98**, 15050-15055.
Musacchio, A. and Salmon, E. D. (2007). The spindle-assembly checkpoint in space and time. *Nat. Rev. Mol. Cell Biol.* **8**, 379-393.
Nystul, T. G., Goldmark, J. P., Padilla, P. A. and Roth, M. B. (2003). Suspended animation in C. elegans requires the spindle checkpoint. *Science* **302**, 1038-1041.
Padilla, P. A. and Roth, M. B. (2001). Oxygen deprivation causes suspended animation in the zebrafish embryo. *Proc. Natl. Acad. Sci. USA* **98**, 7331-7335.
Padilla, P. A., Nystul, T. G., Zager, R. A., Johnson, A. C. and Roth, M. B. (2002). Dephosphorylation of cell cycle-regulated proteins correlates with anoxia-induced suspended animation in Caenorhabditis elegans. *Mol. Biol. Cell* **13**, 1473-1483.
Peset, I., Seiler, J., Sardon, T., Bejarano, L. A., Rybina, S. and Vernos, I. (2005). Function and regulation of Maskin, a TACC family protein, in microtubule growth during mitosis. *J. Cell Biol.* **170**, 1057-1066.
Pouyssegur, J., Dayan, F. and Mazure, N. M. (2006). Hypoxia signalling in cancer and approaches to enforce tumour regression. *Nature* **441**, 437-443.
Raff, J. W., Jeffers, K. and Huang, J. Y. (2002). The roles of Fzy/Cdc20 and Fzr/Cdh1 in regulating the destruction of cyclin B in space and time. *J. Cell Biol.* **157**, 1139-1149.
Savoian, M. S., Gatt, M. K., Riparbelli, M. G., Callaini, G. and Glover, D. M. (2004). Drosophila Klp67A is required for proper chromosome congression and segregation during meiosis I. *J. Cell Sci.* **117**, 3669-3677.
Schittenhelm, R. B., Heeger, S., Althoff, F., Walter, A., Heidmann, S., Mechtler, K. and Lehner, C. F. (2007). Spatial organization of a ubiquitous eukaryotic kinetochore protein network in Drosophila chromosomes. *Chromosoma* **116**, 385-402.
Sciambi, C. J., Komma, D. J., Skold, H. N., Hirose, K. and Endow, S. A. (2005). A bidirectional kinesin motor in live Drosophila embryos. *Traffic* **6**, 1036-1046.
Sharp, D. J., Brown, H. M., Kwon, M., Rogers, G. C., Holland, G. and Scholey, J. M. (2000a). Functional coordination of three mitotic motors in Drosophila embryos. *Mol. Biol. Cell* **11**, 241-253.
Sharp, D. J., Rogers, G. C. and Scholey, J. M. (2000b). Cytoplasmic dynein is required for poleward chromosome movement during mitosis in Drosophila embryos. *Nat. Cell Biol.* **2**, 922-930.
Stucke, V. M., Sillje, H. H., Arnaud, L. and Nigg, E. A. (2002). Human Mps1 kinase is required for the spindle assembly checkpoint but not for centrosome duplication. *EMBO J.* **21**, 1723-1732.
Vader, G., Medema, R. H. and Lens, S. M. (2006). The chromosomal passenger complex: guiding Aurora-B through mitosis. *J. Cell Biol.* **173**, 833-837.
Wadsworth, P. and Salmon, E. D. (1988). Spindle microtubule dynamics: modulation by metabolic inhibitors. *Cell Motil. Cytoskeleton* **11**, 97-105.
Zalokar, M. and Erk, I. (1976). Division and migration of nuclei during early embryogenesis of Drosophila melanogaster. *J. Microsc. Biol. Cell* **25**, 97-109.